CITATION

Münchow, A., K.K. Falkner, H. Melling, B. Rabe, and H.L. Johnson. 2011. Ocean warming of Nares Strait bottom waters off Northwest Greenland, 2003–2009. *Oceanography* 24(3):114–123, http://dx.doi.org/10.5670/oceanog.2011.62.

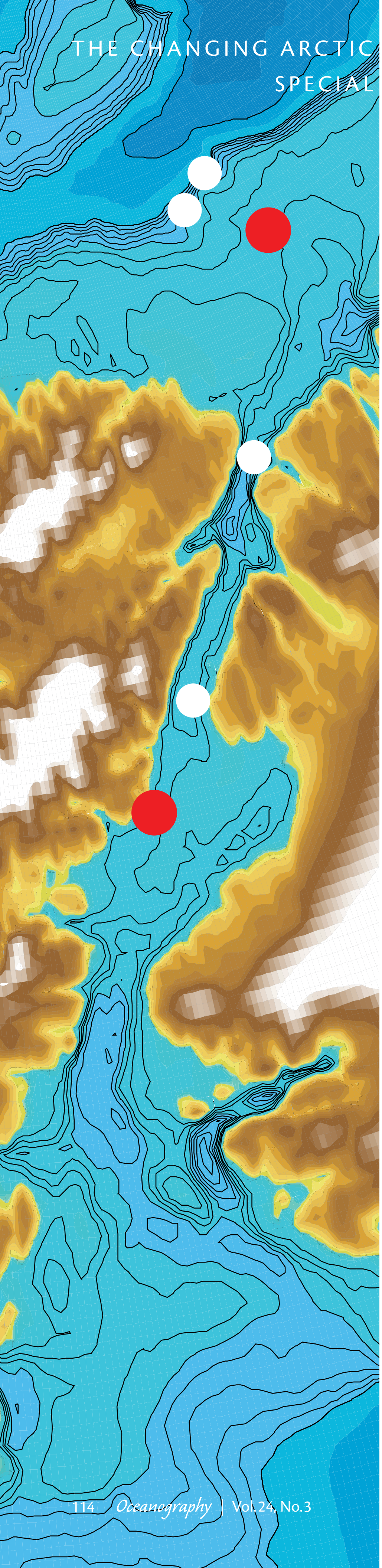

OCEAN WARMING OF NARES STRAIT BOTTOM WATERS

OFF NORTHWEST GREENLAND, 2003–2009

BY ANDREAS MÜNCHOW, KELLY K. FALKNER, HUMFREY MELLING, BERIT RABE, AND HELEN L. JOHNSON

ABSTRACT. Over the last 60 years, the perception of the Arctic Ocean has changed from a hostile, sluggish, steady, ice-covered environment with little global impact to an ocean that has become increasingly accessible, apparently rapidly changing, only partly ice-covered, and connected to the global meridional overturning circulation. Our new observations demonstrate that waters off Northwest Greenland constitute the final limb in the grand cyclonic circulation of the Atlantic layer in the Arctic Ocean. These waters with an Atlantic water mass signature are warming in Nares Strait to the west of Greenland as they are elsewhere. Estimates of the magnitude and uncertainty of this warming are emerging from both moored observations and historical hydrographic station data.

Ocean temperatures sensed by instruments moored 3 m above the bottom between 228 and 366 m depth in Nares Strait suggest a mean warming of about 0.023 ± 0.015°C per year for the 2003–2009 period at 95% confidence. Salinity changes for the same period are not significantly different from zero. Nevertheless, oscillating bottom temperatures covary with salinities. Mean bottom salinities in Nares Strait exceed 34.56 psu while no water with salinities above 34.51 psu occurs in Baffin Bay to the south. These data indicate a dominantly northern source for the waters sensed by our moorings. Mean bottom temperatures hover near 0°C, which suggests minimal influence of waters from the northeastern Amundsen Basin in the Arctic Ocean. Thus, we conclude that the observed warming originates from the northeastern Canadian Basin to the southwest of our study area.

In addition to these mean conditions, we find large interannual variability. For example, significant freshening emerges for the 2003–2006 period that reaches −0.02 ± 0.008 psu per year without significant concurrent temperature trends at three sensor locations. These data contrast with the 2007–2009 observational period when five different sensors all indicate warmer waters (0.063 ± 0.017°C per year) and saltier waters (0.027 ± 0.01 psu per year), which reverses the 2003–2006 freshening. We speculate that some of these observed changes are caused by a changing ice regime. During the 2003–2006 winters, ice was landfast, while during 2007–2009 it was generally mobile year-round. The warming impacts tidewater glaciers along northern Greenland with sill depths below 300 m, for example, Petermann Gletscher.

INTRODUCTION

When a large Northwest Greenland outlet glacier (Petermann Gletscher) discharged an ice island four times the size of Manhattan in August 2010, the United States Congress held formal inquiries on its cause within days of the event. Some scientists and the global media speculated that this event, as well as concurrent severe droughts in Russia and floods in China and Pakistan, were tied to record-breaking air temperatures and global warming. Reviewing available data, Johnson et al. (2011) and Falkner et al. (2011) cautioned that most melting of floating ice shelves such as Petermann Gletscher is dominated by physical ocean processes below, not above, the ice (Rignot and Steffen, 2008). Here, we provide evidence that waters adjacent to Petermann Gletscher (1) originate from the Arctic Ocean to the north, (2) contain heat of Atlantic origin, and (3) have warmed significantly since 2003.

In recent years, changing ocean properties are observed in the Eurasian (Polyakov et al., 2010) and North American (McLaughlin et al., 2009; Melling, 1998) sectors of the Arctic Ocean. Pronounced subsurface temperature maxima (Coachman and Barnes, 1963) in the Arctic Ocean and its marginal seas are the result of inflowing warm, salty Atlantic waters. These waters enter via eastern Fram Strait (Fahrbach et al., 2001) and the Barents Sea (Schauer et al., 2002). The circulation of the central Arctic Ocean is generally cyclonic (counterclockwise) and most intense near boundaries adjacent to sloping topographic features (Nikolopoulos et al., 2008). It is explained elegantly by vorticity conservation in the presence of a wind-stress curl (Yang, 2005). Atlantic layer core temperatures in the Arctic vary from 4°C in the generally ice-free Barents Sea (Levitus et al., 2009) to below 0.5°C in the generally ice-covered eastern Canadian Basin (McLaughlin et al., 2009; Melling, 1998).

The Canadian Archipelago, Fram Strait, and Barents Sea constitute pathways of water, ice, and vorticity between the Arctic and Atlantic Oceans. Arctic outflows via these pathways return freshwaters to the North Atlantic that were evaporated from tropical oceans, transported by the atmosphere, and delivered to the Arctic Ocean via precipitation, terrestrial runoff, and inflow from the North Pacific (Emile-Geay et al., 2003). Other waters of Pacific, Atlantic, and local origin also contribute to circulation. Here, we here focus on changing water properties in Nares Strait to the west of Greenland bordering the Canadian Archipelago (Münchow et al., 2007). Nares Strait is a major conduit of southward flux into Baffin Bay and the Atlantic Ocean (Münchow and Melling, 2008). Fluxes and properties through Nares Strait reflect the impacts of disintegrating ice shelves of northern Canada (Copland et al., 2007), potentially surging glaciers of northern Greenland (Rignot and Steffen, 2008; Johnson et al., 2011), and diminishing sea ice in the Arctic (Parkinson and Cavalieri, 2008).

Because the Lincoln Sea, to the north of Greenland and Ellesmere Island, contains some of the oldest and thickest ice anywhere in the Arctic Ocean, the circulation and properties of its underlying waters impact the fate of these last remains of multiyear ice. The flux of such ice is currently limited to a three-to-four-month-long summer season. For the remainder of the year, the ice is landfast, but the duration of these conditions are changing (Kwok et al., 2010). More specifically, the length of the landfast ice season in winter is decreasing. Processes within and adjacent to the Canadian Archipelago strongly link ice, ocean, and land in a system that conceivably moves more multiyear ice from the Arctic than is currently possible during a three-to-four month season of ice mobility.

Subsurface Arctic Ocean temperature records longer than 80 years reveal both multidecadal oscillations (Levitus et al., 2009; Polyakov et al., 2004) and smaller, but significant, linear trends of increasing temperatures (Polyakov et al., 2004; Zweng and Münchow, 2006). Analyses of discrete hydrographic ship surveys such as those cited are challenged by seasonally biased sampling, gappy records, and aliasing introduced by unresolved spatial and temporal variabilities of a dynamical ice-ocean-atmosphere system (Wunsch and Heimbach, 2006). In contrast, generally shorter mooring records sample more frequently and with a constant time step, and thus contain less bias, but to date mooring records are shorter than a decade.

Here, we introduce temperature and salinity measurements from moorings that describe means, variability, and trends from supertidal to interannual time scales near the bottom at several locations across a 38 km wide section of Nares Strait from 2003 to 2009. After introducing our study area to the west of Greenland, we place our moored measurements into a larger spatial context with discrete vertical profiles collected from ships and helicopters in 2003. Time series of bottom temperature and salinity are analyzed for dominant time scales of variability as well as

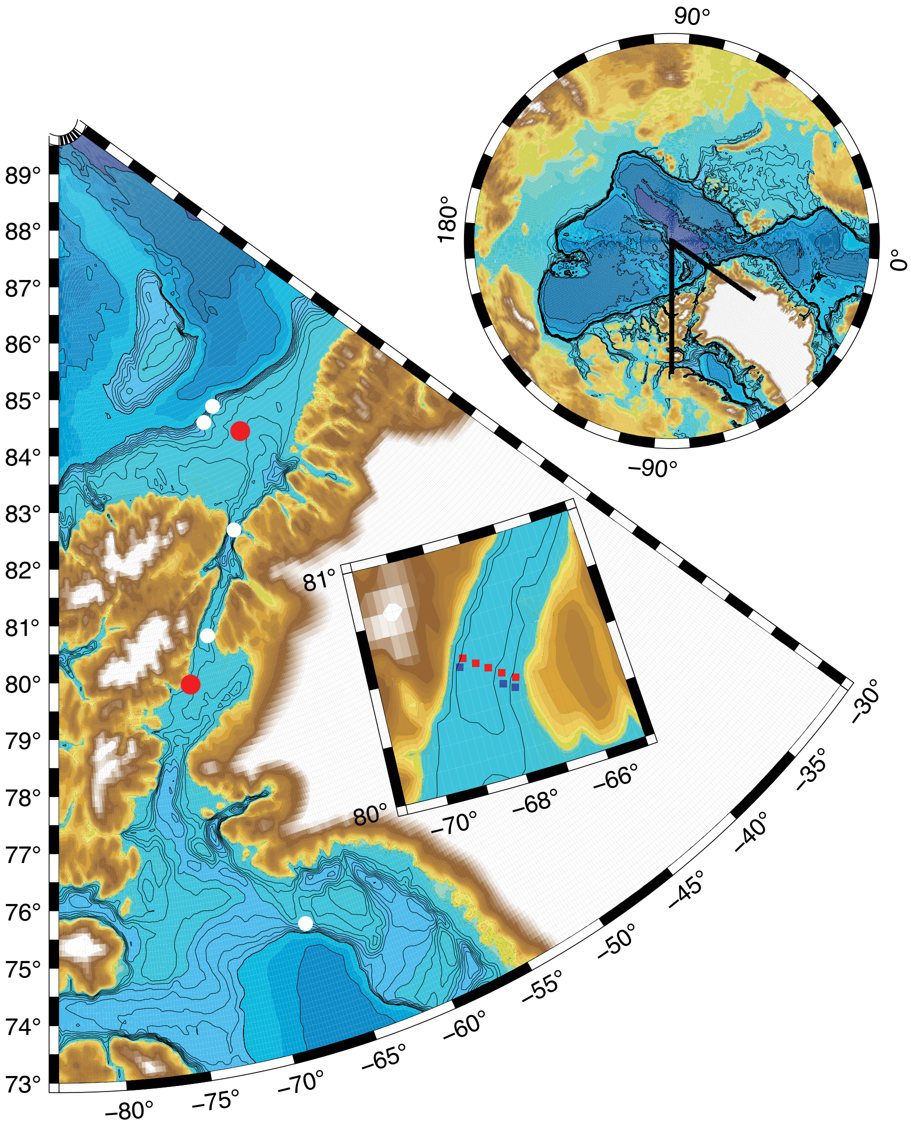

Figure 1. Maps of the Arctic Ocean (top right) and Nares Strait (bottom left) study area with bottom contours from IBCAO (http://www.ngdc.noaa.gov/mgg/bathymetry/arctic) in meters, with contours every 100 m from 200 to 1000 m, and 1000 m beyond that depth. Sill locations are indicated with large red circles in the north (290 m) and south (225 m). White circles indicate locations of selected 2003 conductivity-temperature-depth (CTD) casts. The inset near 80.5°N indicates bottom-mounted acoustic Doppler current profiler mooring locations for 2003–2006 (blue symbols for KS02, KS10, KS12 from west to east) and 2007–2009 (red symbols for KS04, KS06, KS08, KS10, and KS12 from west to east), the symbols for the 2003–2006 mooring locations are offset by 0.05° latitude from their true location for clarity.

for linear trends that constitute a first estimate of variations at decadal time scales. We discuss our findings in the context of both multidecadal oscillations and a potential regime change toward an Arctic with a more seasonal and mobile ice cover.

DATA SOURCES

Starting in 2003, we measured ocean properties in Nares Strait, a 30–50 km wide waterway that separates Greenland from Canada between 78°N and 83°N (Figure 1). To the north it connects to the Arctic Ocean, while to the south it connects to Baffin Bay and subsequently the Atlantic Ocean. At 80.5°N we deployed an array of moorings to measure ocean currents, temperature, and conductivity across a 38 km wide and 350 m deep section of Nares Strait. Münchow and Melling (2008) and Rabe et al. (2010) introduced details and first results from instruments measuring ocean currents between 30 m and 300 m depth and temperature, conductivity, and pressure between 30 m depth and a few meters above the seabed for the 2003–2006 period. The instruments recovered in 2006 and 2009 provide gap-free records that are three and two years long, respectively. Here, we report for the first time on interannual temperature and salinity changes for the 2003–2009 period.

Bottom-mounted Sea-Bird 37SM sensors reveal temperature and salinity about 3 m above the bottom where turbulence levels, biological activity, and mooring motions are all smaller than in the water column above. Samples were taken every 15 minutes. Salinity is estimated from conductivity, temperature, and pressure. We estimate temporal sensor drift by comparing 20 days of

Andreas Münchow *(muenchow@udel.edu) is Associate Professor, College of Earth, Ocean and Environment, University of Delaware, Newark, DE, USA.* **Kelly K. Falkner** *is Deputy Director, Office of Polar Programs, National Science Foundation, Arlington, VA, USA.* **Humfrey Melling** *is Senior Researcher, Fisheries and Oceans Canada, Institute of Ocean Sciences, Sidney BC, Canada.* **Berit Rabe** *is a scientist at Marine Laboratory, Marine Scotland Science, Aberdeen, UK.* **Helen L. Johnson** *is Royal Society University Research Fellow, Department of Earth Sciences, University of Oxford, Oxford, UK.*

mooring records at the start and the end of the series with discrete vertical conductivity-temperature-depth (CTD) profiles taken during deployment and recovery operations. Assuming negligible drift of temperature sensors, we find (not shown) that salinities drift by about 0.051 psu toward fresher values for the 2003–2006 period (–0.017 psu yr^{-1}) and 0.031 psu toward fresher values also for the 2007–2009 period (–0.016 psu yr^{-1}). The sign and magnitude of these changes is consistent with gradual fouling of a conductivity cell. This constant salinity drift is removed from the 2003–2006 records at KS02, KS10, and KS12 as well as from the 2007–2009 records at KS04, KS06, KS08, KS10, and KS12 (see Figure 1 for locations).

Of the eight separate time series of salinity S, only two records contain salinity spikes with $S < 34.1$ psu. Both occur at KS10 with the first starting May 16, 2005, lasting for 18 days, and the second starting November 26, 2008, lasting 0.25 days. We replaced these anomalous salinities with values estimated from a linear regression of salinity against temperature 10 days prior. As a final processing step, we applied a Lanczos raised cosine low-pass filter with a half-power point near 34 hours to remove tidal and inertial variations. Uncertainties in statistical estimates require knowledge of the degrees of freedom, the ratio of the record length T to the decorrelation time scale T_d. We determine T_d by integrating lagged autocorrelations of salinity and temperature to their first zero crossing and find T_d in the range of 5–14 days (not shown). Using T_d = 14 days, our 2003–2006 and 2007–2009 records have about 78 and 51 degrees of freedom.

SPATIAL CONTEXT

Figure 1 shows the location of our larger study area from the 4,000 m deep Amundsen Basin and 1,500 m deep Lomonosov Ridge in the Arctic Ocean at 89°N to the 2,000 m deep Baffin Bay basin at 73°N. Nares Strait connects these two basins with northern and southern sill depths near 84°N and 80°N of about 300 m and 200 m depth, respectively. Figure 1 also shows the location of five CTD casts that were taken in Nares Strait between its northern and southern sills as well as stations bordering the adjacent deep basins to the north and south of the sills. Figure 2 depicts vertical profiles of salinity from 150 m below the surface to the bottom near 500 m depth. Below the main halocline at any given depth, the data clearly show the progression of high salinities in the Arctic Ocean to lower salinities in Nares Strait and to the lowest salinities in Baffin Bay. Except for Baffin Bay, the correlation of salinity S with potential temperature θ is almost linear (Figure 3) as temperature increases with salinity. All Nares Strait waters with salinities above 34.54 are either locally produced by brine injections or must have entered from the north, because Baffin Bay waters with a subsurface temperature maximum have salinities that are always less than 34.54 (recent work of authors Münchow, Falkner, and Melling).

The shallow Nares Strait cast terminating at 330 m depth with a bottom salinity of 34.72 psu originates from our mooring section, while a deeper Nares Strait cast taken to the north measures salinities reaching 34.82 psu at 500 m. Waters with these θ-S characteristics refer to water masses that have fixed temperature (θ) and salinity (S) characteristics and are found at about 350 m depth in the Arctic Ocean just to the north of the northern sill. These data indicate that either an uncharted sill deeper than the charted 300 m sill exists or episodic upwelling raises the salty Arctic Ocean waters from 350 m to 300 m depth and over the

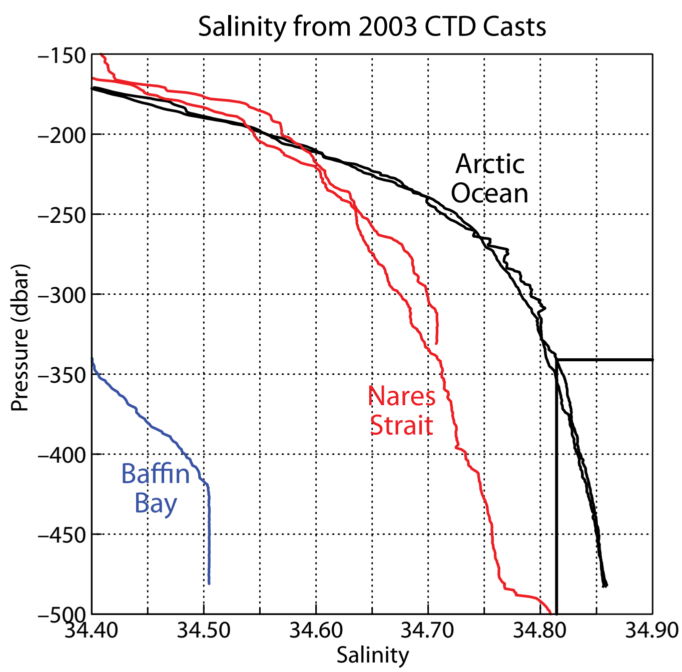

Figure 2. Vertical salinity profiles below 150 m from the Arctic Ocean to the north of the northern sill (black), Nares Strait between the northern and southern sill (red), and Baffin Bay to the south of the southern sill (blue). See Figure 1 for locations. The Nares Strait profile terminating near 330 dbar originates from our mooring section, while the profile terminating at 500 dbar is to the north where the densest water occurred in 2003 (σ_θ = 27.94 kg m^{-3}, S = 34.82 psu).

sill to subsequently cascade down into Nares Strait to form Nares Strait bottom water with $S = 34.82$ psu and $\theta = 0.20$°C. The vertical excursion would likely be larger than 50 m as the downward motion would entrain fresher water as it descends.

In addition to the temperature-salinity correlations from the CTD casts, Figure 3 shows the mean temperature and salinity values from the eight time series (Table 1) along with the magnitude of temperature and salinity changes discussed next. Mean values aggregate between 34.56 psu and 34.67 psu along the Arctic Ocean and Nares Strait correlations. These data give confidence that both the 2003 CTD casts and our mooring data represent similar waters.

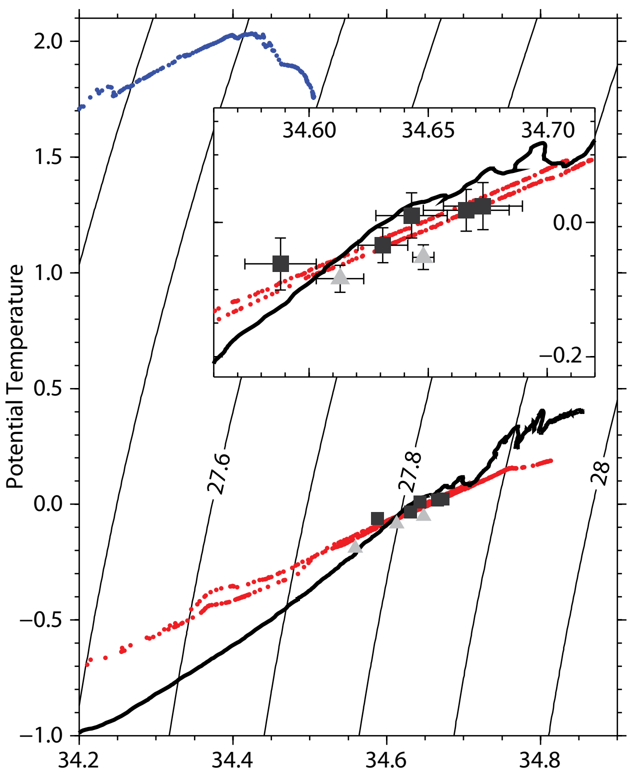

Figure 3. Temperature-salinity correlations from the Arctic Ocean to the north of the northern sill (black), Nares Strait between the northern and southern sill (red), and Baffin Bay to the south of the southern sill depth (blue). Symbols represent record mean properties of eight mooring records in the range [34.56, 34.67] psu for salinity and [−0.19, +0.10] °C for temperature (Table 1) with triangles from the 2003–2006 and rectangles from the 2007–2009 deployments. See Figure 1 for locations. Contours are lines of constant density. The insert is an expanded view where the uncertainties represent changes about the mean associated with changes discussed in the text.

TIME SERIES 2003–2009

Figure 4 shows salinity and potential temperature for the 2003–2006 and 2007–2009 deployments near the center of the channel at KS10 (see Figure 1 for location). Salinity at KS10 generally varies between 34.4 psu and 34.7 psu except for two events in January 2004 (Day 366) and December 2007 (Day 1,800) with unfiltered salinities reaching almost 34.3 psu that also correspond to lower temperatures (not shown). Temperatures are within a narrow range between −0.4°C and +0.2°C except for two short events. Without the hindsight of mooring data, Samelson et al. (2006) discuss the first event in terms of strong wind forcing and ice motion that Rabe (2010) analyzes as the wind-driven response of a density-stratified channel flow under the influence of rotation. The perhaps physically similar 2007 event of low bottom temperature and salinity also corresponds to strong winds from

Table 1. Mooring details, averaged temperature T_{avg} and salinity S_{avg}, linear trend for temperature dT/dt and salinity dS/dt, along with 95% confidence levels assuming a 14-day decorrelation time scale resulting in 78 and 51 degrees of freedom for the 2003–2006 and 2007–2009 deployments, respectively.

Name	Longitude (°W)	Latitude (°N)	Depth (m)	T_{avg} (°C)	S_{avg} (psu)	dT/dt, °C/year	dS/dt, psu/year
KS02 2003-06	68.874	80.554	302	−0.19	34.56	−0.010 ± 0.014	−0.018 ± 0.008
KS10 2003-06	67.930	80.439	299	−0.05	34.65	+0.000 ± 0.020	−0.015 ± 0.010
KS12 2003-06	67.671	80.409	263	−0.08	34.61	+0.001 ± 0.025	−0.026 ± 0.014
KS04 2007-09	68.739	80.538	366	−0.03	34.64	+0.065 ± 0.022	+0.030 ± 0.013
KS06 2007-09	68.456	80.504	358	+0.02	34.67	+0.063 ± 0.028	+0.035 ± 0.016
KS08 2007-09	68.185	80.472	356	+0.02	34.67	+0.066 ± 0.029	+0.028 ± 0.017
KS10 2007-09	67.893	80.436	293	+0.01	34.64	+0.059 ± 0.037	+0.023 ± 0.022
KS12 2007-09	67.593	80.399	228	−0.06	34.59	+0.064 ± 0.047	+0.019 ± 0.030

the north. These winds cause strong upwelling off Greenland that brings warmer waters toward the surface and advects loose ice toward the channel center and to the south (Rabe, 2010). This upwelling results in large areas of active sea ice formation that is visible in MODIS (Moderate Resolution Imaging Spectroradiometer) thermal imagery (Figure 5), where high brightness temperatures indicate thermal radiation from open water or thin ice.

Note that the highest salinities with values above 34.7 psu occur at the beginning of the record in the summer of 2003 and the end of the record in the summer of 2009. Salinities indicate that waters become fresher in 2003 and saltier in 2009 for six to nine months. Within a time series covering six years, such short-period trends stand out, but they are balanced by opposing trends at other times. A single year-long record, however, would potentially misinterpret the significance of such trends that really are oscillations at time scales longer than the record. The same caveat, albeit at decadal time scales, applies to any linear trend analysis applied to our six-year period of observation.

LINEAR REGRESSIONS

Table 1 lists record mean values and salient statistics for each location for each deployment period. The linear warming and freshening during the period of observation are overlaid in Figure 4 for the center of the channel at KS10 for potential temperature θ and salinity S both as time series and as θ-S scatter. The linear trend line for time series is also shown with values for the slopes listed in Table 1. Furthermore, we color code data prior to May 16, 2005, (Day 866) in black and those after this time in red for the 2003–2006 record. While not apparent from the time series, depicting the data as θ-S scatter irrespective of time, we show that the selected time corresponds to the arrival of a fresher and warmer water mass.

More specifically, a strong linear relation exists in θ-S space; however, the relation prior and after May 16, 2005, is distinct. Furthermore, this shift occurs instantaneously at multiple bottom sensors across the section, such as at

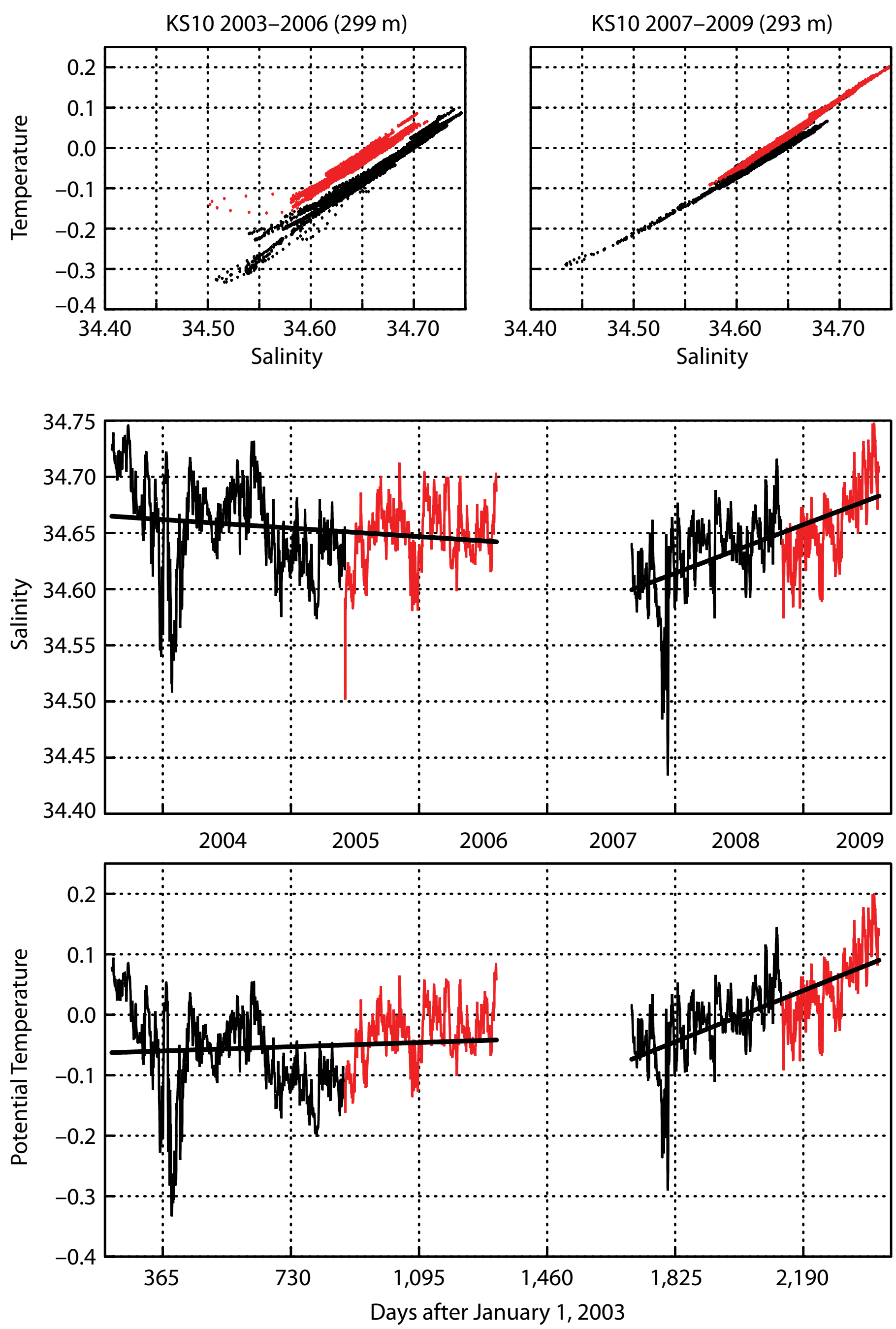

Figure 4. Time series and correlations of salinity and potential temperature near the bottom at KS10. Data are low-pass filtered to remove tidal and inertial variability. Different colors indicate data relative to events discussed in the text.

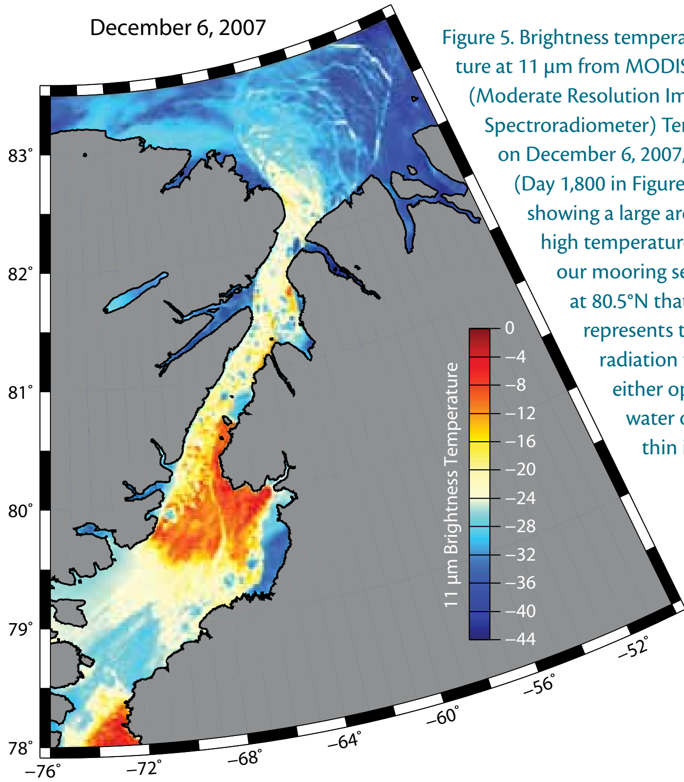

Figure 5. Brightness temperature at 11 µm from MODIS (Moderate Resolution Imaging Spectroradiometer) Terra on December 6, 2007, (Day 1,800 in Figure 4) showing a large area of high temperatures near our mooring section at 80.5°N that represents thermal radiation from either open water or very thin ice.

KS02 adjacent to the coast of Canada (Figure 6) and at KS12 near the coast of Greenland (not shown). This date separates cooler, fresher water from warmer, saltier water. Similar coherent changes of water properties across the entire array occur during the 2007–2009 deployments on October 31, 2008, which Figures 4 and 5 show for the center channel location KS10 and a coastal Canada location KS04. Additional sensors at KS06, KS08, and KS12 show similar behavior (Table 1).

During the 2003–2006 period, linear trends of potential temperature θ are indistinguishable from zero with 95% confidence levels at all three locations across the channel (Table 1). In contrast, salinity trends indicate freshening of about 0.018 ± 0.008 psu per year at KS02 (Figure 6). Values at all three locations are indistinguishable from each other within their respective uncertainties, which is true for the 2007–2009 period as well. For the latter period, however, our data suggest more dramatic rates of change in time. Both temperature and salinity trends are different from zero at 95% confidence except for one shallower location (KS12). At KS04, temperature and salinity trends exceed 0.065 ± 0.022°C per year and 0.030 ± 0.013 psu per year (Figure 6). There is no apparent pattern in these rates from sensor to sensor across the channel. We thus assume that each record represents an independent realization of the same change. This reduces the uncertainty of the estimated across-channel averaged trends by $\sqrt{N-1}$ where N = 3 for 2003–2006 and N = 5 for 2007–2009. Sectionally averaged bottom temperature in Nares Strait thus warms by 0.027 ± 0.010°C and becomes saltier by 0.063 ± 0.017 psu per year from 2007 to 2009.

DISCUSSION

The Arctic Ocean resembles an estuary with respect to the Atlantic Ocean. As a strongly stratified ocean, it delivers relatively fresh waters to the Atlantic near the surface and in return receives relatively salty waters below the surface. Both the Arctic's sea ice cover and the stability of Greenland's outlet glaciers depend on the delicate balance of the inflows and outflows and the salt and heat content that these waters carry.

Analysis of historical records of ship-based observations indicates Arctic change in temperature and salinity for the last 10–100 years (Melling, 1998; Polyakov et al., 2004; Zweng and Münchow, 2006; Levitus et al., 2009; McLaughlin et al., 2009). Most of these records contain linear trends that demonstrate subsurface warming of the Atlantic layer. The data also contain large amounts of scatter and oscillations. Furthermore, much of the sampling is seasonally biased toward the polar summers when access is easier. Few records include frequent enough sampling to resolve temporal and spatial oscillations due to Kelvin and Rossby waves (Gill, 1982) that have periods of days to months. And lastly, few historical records are long enough to resolve interannual and decadal oscillations of atmospheric circulation patterns described by the North Atlantic Oscillation (Hurrell and Deser, 2009) and the Atlantic Multidecadal Oscillation (Enfield et al., 2001).

Exceptions are Levitus et al. (2009) who find strong correlations in an almost 110-year-long record of subsurface Barents Sea temperature measurements that correlate with the Atlantic Multidecadal Oscillation. Polyakov et al. (2004) report Atlantic layer core temperatures from Arctic Ocean slopes and basins. The authors also find correlations with climate indices in addition to a weak background warming trend of 0.026 ± 0.008°C per decade for the region north of Nares Strait from discrete casts covering 26 different years with data. Note that this trend is an order of magnitude smaller than what we report here for our 2003–2009 mooring record and that the 26 CTD casts are widely separated in both time and space.

We report here the first results from moored records that for five years resolved hourly to interannual time scales at 5 km spatial scales. Our array does not resolve decadal variability, but the linear trend represents a first estimate of long-term variability that includes both decadal variability and steady background warming or cooling. We are presently unable to distinguish between the two. Nevertheless, combining our 2003–2006 and 2007–2009 records from three and five sensors, respectively, we find a mean warming of about 0.023 ± 0.015°C per year where the uncertainty represents a 95% confidence interval for a 14-day decorrelation time scale determined conservatively from the data. The salinity data reveal freshening of –0.001 ± 0.009 psu per year that is not significantly different from zero.

The observed trends are spatially coherent across the section. The large warming by up to 0.07°C per year starting in 2007 coincides with the arrival of waters that also exhibit higher salinities that reversed the freshening of prior years. Water properties in Nares Strait also change at daily to interannual times scales, perhaps associated with the arrival of water mass fronts in θ space. The timing and frequency of such occurrences contribute to the warming but imply a different and potentially more dynamic and nonlinear process than a steady, uniform, linear rise of ocean temperatures.

We present two speculations on the cause of the enhanced warming, namely (1) advection from the north, and (2) local convection with attendant vertical mixing. First, warming waters of Atlantic origin previously detected in the Canada Basin (McLaughlin et al., 2009) may have reached the Lincoln Sea, pushed over the 300 m deep

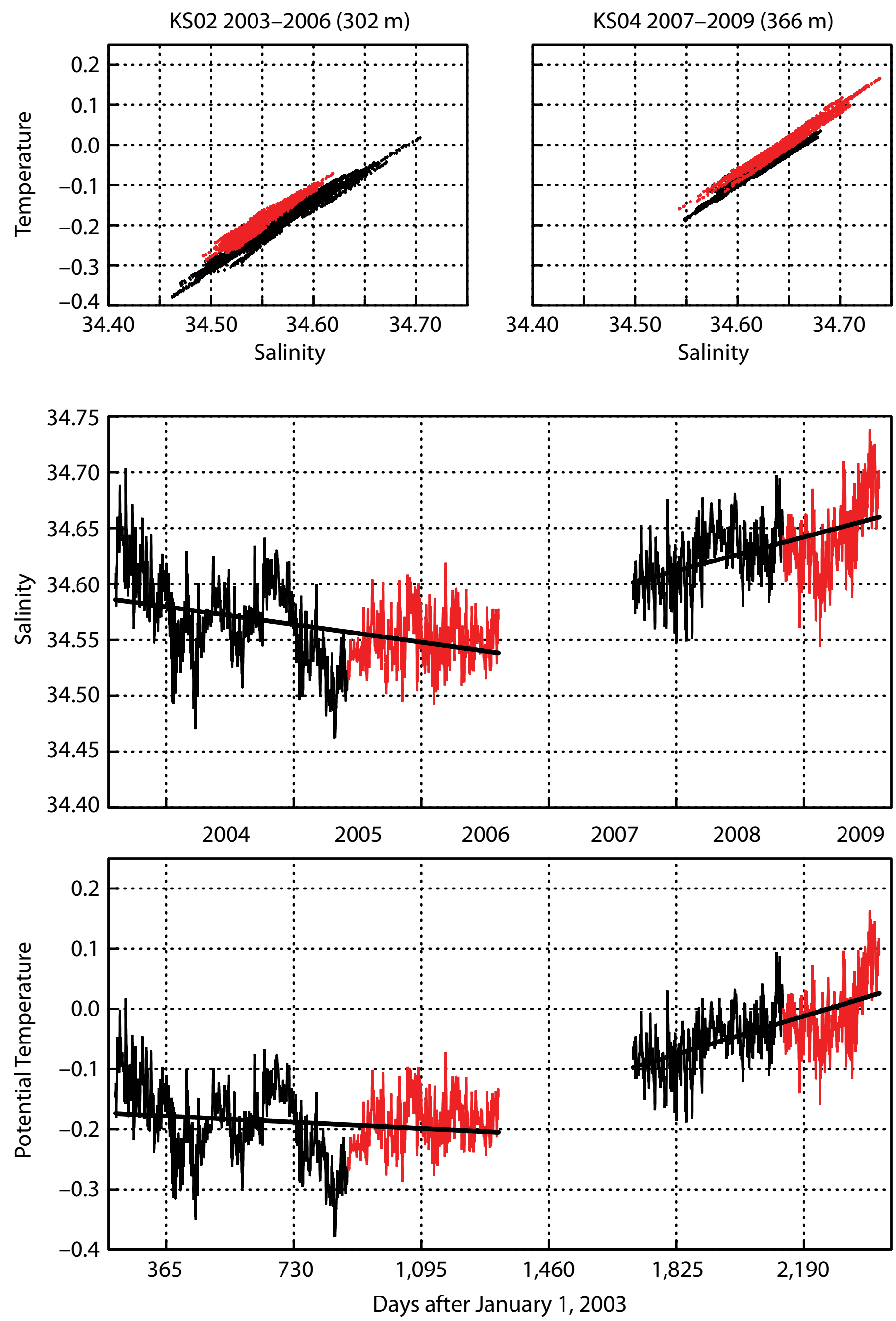

Figure 6. Time series and correlations of salinity and potential temperature near the bottom at KS02 for 2003–2006 and KS04 for 2007–2009. Data are low-pass filtered to remove tidal and inertial variability. Different colors indicate data relative to events discussed in the text.

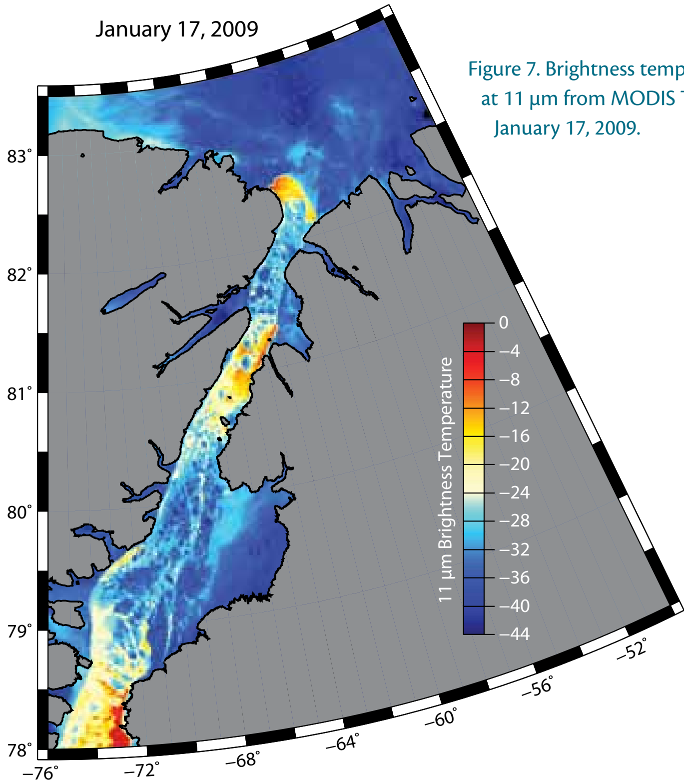

Figure 7. Brightness temperature at 11 µm from MODIS Terra on January 17, 2009.

northern sill, and entered Nares Strait from the north. Bottom temperature and salinity in Nares Strait suggest a source for such water at 350 m depth in the Arctic Ocean. In order to enter Nares Strait, these waters must be lifted intermittently by almost 50 m to cross the sill and plunge to the bottom of Nares Strait (Figure 2).

A second, perhaps concurrent, cause could be changing local ice conditions. More specifically, for the 2003–2006 period, Nares Strait developed ice arches at its southern entrance (Dumont et al., 2009) that remained in place for 158, 242, and 169 days during the three winters (Kwok et al., 2010). This arch locks all motion of ice in Nares Strait (Dunbar, 1973), decouples the ocean circulation from the local atmosphere, and supports the North Water polynya (Melling et al., 2001). The polynya failed to form in the 2006/07 winter (Münchow et al., 2007) when ice was moving all year through Nares Strait from north to south. During the 2007/08 winter, it lasted for only 68 days (Kwok et al., 2010), and it again failed to form at all in the winter of 2008/09. Instead, a northern ice arch formed on January 17, 2009 (Figure 7) and all locally produced sea ice was promptly exported into Baffin Bay to the south. This northern ice arch formation coincided with a rapid warming observed in 2009 at all locations in Nares Strait both near the bottom (Figure 4) and within the water column (not shown). Year-long southward advection of ice and surface waters leads to enhanced local ice production, brine rejection, and entrainment of overlying warm waters as these brines sink. This process may be further enhanced during periods of strong upwelling-favorable winds from the north. The offshore Ekman transport off Greenland due to winds from the north moves loose or thin ice toward the center of the channel. Thus, the open waters created during freezing air temperatures result in enhanced sea ice production, brine rejection, and entrainment of overlying warm waters as these brines sink (Figure 7).

MODIS thermal imaging for the 2009/10 winter (not shown) indicates that a northern ice arch similar to that shown in Figure 7 formed intermittently without a southern ice arch. A southern ice arch formed on January 30 and persisted through June 30, 2011 (not shown) for the first time since 2006 except for a short 2 month period in 2008. An array of bottom-moored sensors was deployed in Nares Strait in 2009 that will hopefully be recovered in 2012 to extend our ocean observations for another three years. We hypothesize that the accelerated large warming trend coincident with the failure of a southern ice arch will have continued through 2010 but will reverse in 2011. The fact that we find statistically significant regressions indicative of freshening for the 2003–2006 and increasing salinity for the 2007–2009 periods should encourage (1) cautious interpretations of short records and (2) efforts to extend existing interannual observations at key locations such as Nares Strait. Such data are crucial for testing Arctic Ocean and climate models under development with sufficient resolution to more faithfully represent flows and driving forces through the Canadian Archipelago and adjacent waters.

ACKNOWLEDGMENTS

We are grateful to the officers and crews of USCGC *Healy* commanded by Captain Dan Oliver and CCGS *Henry Larsen* commanded by Captains John

Vanthiel and John Broderick, who endorsed our scientific objectives with enthusiastic professionalism as did a dedicated group of students, technicians, and engineers. The work was funded by the National Science Foundation under grants 0230236 (AM, HM, BR), 1022843 (AM), 0230354 (KKF) as well as the Canadian International Polar Year project 2006-SR1-CC-135 (HM).

REFERENCES

Coachman, L., and C. Barnes. 1963. The movement of Atlantic water in the Arctic Ocean. *Arctic* 16:9–16.

Copland, L., D.R. Mueller, and L. Weir. 2007. Rapid loss of the Ayles ice shelf, Ellesmere Island, Canada. *Geophysical Research Letters* 34, L21501, http://dx.doi.org/10.1029/2007GL031809.

Dumont, D., Y. Gratton, and T.E. Arbetter. 2009. Modeling the dynamics of the North Water polynya ice bridge. *Journal of Physical Oceanography* 39:1,448–1,461, http://dx.doi.org/10.1175/2008JPO3965.1.

Dunbar, M. 1973. Ice regime and ice transport in Nares Strait. *Arctic* 26:282–291.

Emile-Geay, J., M.A. Cane, N. Naik, R. Seager, A.C. Clement, and A. van Geen. 2003. Warren revisited: Atmospheric freshwater fluxes and "why is no deep water formed in the North Pacific." *Journal of Geophysical Research* 108, 3178, http://dx.doi.org/10.1029/2001JC001058.

Enfield, D.B., A.M. Mestas-Nunez, and P.J. Trimble. 2001. The Atlantic multidecadal oscillation and its relation to rainfall and river flows in the continental US. *Geophysical Research Letters* 28:2,077–2,080, http://dx.doi.org/10.1029/2000GL012745.

Fahrbach, E., J. Meincke, S. Osterhus, G. Rohardt, U. Schauer, V. Tverberg, and J. Verduin. 2001. Direct measurements of volume transports through Fram Strait. *Polar Research* 20:217–224, http://dx.doi.org/10.1111/j.1751-8369.2001.tb00059.x.

Falkner, K., H. Melling, A.M. Münchow, J.E. Box, T. Wohlleben, H.L. Johnson, P. Gudmandsen, R. Samelson, L. Copland, K. Steffen, and others. 2011. Context for the recent massive Petermann Glacier calving event. *Eos, Transactions, American Geophysical Union* 92(14), http://dx.doi.org/10.1029/2011EO140001.

Gill, A. 1982. *Atmosphere-Ocean Dynamics*. Academic Press Inc., 662 pp.

Hurrell, J.W., and C. Deser. 2009. North Atlantic climate variability: The role of the North Atlantic Oscillation. *Journal of Marine Systems* 78:28–41, http://dx.doi.org/10.1016/j.jmarsys.2008.11.026.

Johnson, H., A. Münchow, K. Falkner, and H. Melling. 2011. Ocean circulation and properties in Petermann Fjord, Greenland. *Journal of Geophysical Research* 116, C01003, http://dx.doi.org/10.1029/2010JC006519.

Kwok, R., L.T. Pedersen, P. Gudmandsen, and S.S. Pang. 2010. Large sea ice outflow into the Nares Strait in 2007. *Geophysical Research Letters* 37, L03502, http://dx.doi.org/10.1029/2009GL041872.

Levitus, S., G. Matishov, D. Seidov, and I. Smolyar. 2009. Barents Sea multidecadal variability. *Geophysical Research Letters* 36, L19604, http://dx.doi.org/10.1029/2009GL039847.

McLaughlin, F.A., E.C. Carmack, W.J. Williams, S. Zimmermann, K. Shimada, and M. Itoh. 2009. Joint effects of boundary currents and thermohaline intrusions on the warming of Atlantic water in the Canada Basin, 1993–2007. *Journal of Geophysical Research* 114, C00A12, http://dx.doi.org/10.1029/2008JC005001.

Melling, H. 1998. Hydrographic changes in the Canada Basin of the Arctic Ocean, 1979–1996. *Journal of Geophysical Research* 103:7,637–7,645, http://dx.doi.org/10.1029/97JC03723.

Melling, H., Y. Gratton, and G. Ingram. 2001. Ocean circulation within the North Water polynya of Baffin Bay. *Atmosphere-Oceans* 39:301–325, http://dx.doi.org/10.1080/07055900.2001.9649683.

Münchow, A., and H. Melling. 2008. Ocean current observations from Nares Strait to the west of Greenland: Interannual to tidal variability and forcing. *Journal of Marine Research* 66(6):801–833.

Münchow, A., K. Falkner, and H. Melling. 2007. Spatial continuity of measured seawater and tracer fluxes through Nares Strait, a dynamically wide channel bordering the Canadian Archipelago. *Journal of Marine Research* 65(6):759–788, http://dx.doi.org/10.1357/002224007784219048.

Nikolopoulos, A., R. Pickart, P. Fratantoni, K. Shimada, D. Torres, and E. Jones. 2008. The western Arctic boundary current at 152°W: Structure, variability, and transport. *Deep-Sea Research Part II* 56:1,164–1,181, http://dx.doi.org/10.1016/j.dsr2.2008.10.014.

Parkinson, C.L., and D.J. Cavalieri. 2008. Arctic sea ice variability and trends, 1979–2006. *Journal of Geophysical Research* 113, C07003, http://dx.doi.org/10.1029/2007JC004558.

Polyakov, I.V., G.V. Alekseev, L.A. Timokhov, U.S. Bhatt, R.L. Colony, H.L. Simmons, D. Walsh, J.E. Walsh, and V.F. Zakharov. 2004. Variability of the intermediate Atlantic water of the Arctic Ocean over the last 100 years. *Journal of Climate* 17:4,485–4,497, http://dx.doi.org/10.1175/JCLI-3224.1.

Polyakov, I.V., L.A. Timokhov, V.A. Alexeev, S. Bacon, I.A. Dmitrenko, L. Fortier, I.E. Frolov, J.-C. Gascard, E. Hansen, V.V. Ivanov, and others. 2010. Arctic ocean warming contributes to reduced polar ice cap. *Journal of Physical Oceanography* 40:2,743–2,756, http://dx.doi.org/10.1175/2010JPO4339.1.

Rabe, B. 2010. Dynamical analysis of flows through Nares Strait, between the Canadian Arctic Archipelago and NW Greenland. PhD thesis, University of Delaware.

Rabe, B., A. Münchow, H. Johnson, and H. Melling. 2010. Nares Strait hydrography and salinity field from a 3-year moored array. *Journal of Geophysical Research* 115, C07010, http://dx.doi.org/10.1029/2009JC005966.

Rignot, E., and K. Steffen. 2008. Channelized bottom melting and stability of floating ice shelves. *Geophysical Research Letters* 35, L02503, http://dx.doi.org/10.1029/2007GL031765.

Samelson, R.M., T. Agnew, H. Melling, and A. Münchow. 2006. Evidence for atmospheric control of sea-ice motion through Nares Strait. *Geophysical Research Letters* 33, L02506, http://dx.doi.org/10.1029/2005GL025016.

Schauer, U., H. Loeng, B. Rudels, V.K. Ozhigin, and W. Dieck. 2002. Atlantic Water flow through the Barents and Kara Seas. *Deep-Sea Research Part I* 49:2,281–2,298, http://dx.doi.org/10.1016/S0967-0637(02)00125-5.

Wunsch, C., and P. Heimbach. 2006. Estimated decadal changes in the North Atlantic meridional overturning circulation and heat flux 1993–2004. *Journal of Physical Oceanography* 36:2,012–2,024, http://dx.doi.org/10.1175/JPO2957.1.

Yang, J.Y. 2005. The Arctic and subarctic ocean flux of potential vorticity and the Arctic Ocean circulation. *Journal of Physical Oceanography* 35:2,387–2,407, http://dx.doi.org/10.1175/JPO2819.1.

Zweng, M.M., and A. Münchow. 2006. Warming and freshening of Baffin Bay, 1916–2003. *Journal of Geophysical Research* 111, C07016, http://dx.doi.org/10.1029/2005JC003093.